Title

CHEMISTRY AND MORPHOLOGY OF COAL LIQUEFACTION. Final Report: Oct. 1, 1983 - Sept. 3, 1984

Author

Heinemann, H.

Publication Date

1984-10-01

LBL-18456
UC-90d

Lawrence Berkeley Laboratory

UNIVERSITY OF CALIFORNIA

Materials & Molecular Research Division

CHEMISTRY AND MORPHOLOGY OF COAL LIQUEFACTION
Annual Report: October 1, 1983 - September 30, 1984

H. Heinemann

October 1984

Prepared for the U.S. Department of Energy under Contract DE-AC03-76SF00098

DISCLAIMER

ANNUAL REPORT

October 1, 1983 - September 30, 1984

CHEMISTRY AND MORPHOLOGY OF COAL LIQUEFACTION

Contract ET-78G-01-3425
4006/6068

Principal Investigator: Heinz Heinemann
Lawrence Berkeley Laboratory
University of California
Berkeley, CA 94720

This work was jointly supported by the Director, Office of Energy Research, Office of Basic Energy Sciences, Chemical Sciences Division, and the Assistant Secretary for Fossil Energy, Office of Coal Research, Liquefaction Division of the U. S. Department of Energy under Contract DE-AC03-76SF00098 through the Pittsburgh Energy Technology Center, Pittsburgh, PA.

CONTENTS

I. INTRODUCTION

The present report covers progress in Tasks 1, 3 and 5 of the original program. Tasks 2, 4 and 6 were discontinued after fiscal year 1982. Task 1 has been completed in fiscal year 1984. Task 3 will be transferred in fiscal year 1985 from funding by the Liquefaction Division of the DOE Office of Coal Research to funding by the Gasification Division, while Task 5 will continue to be funded by the Liquefaction Division. Support by the Director, Office of Energy Research, Office of Basic Energy Sciences, Chemical Sciences Division will terminate at the end of fiscal year 1984. The past support of the various DOE offices is appreciated.

II. Technical Program for FY 1984

Task 1: SELECTIVE SYNTHESIS OF GASOLINE-RANGE COMPONENTS FROM SYNTHESIS GAS

A. T. Bell, Task Manager

It is planned to complete the objectives of the present project during FY 1984. The experimental results obtained for Fischer-Tropsch synthesis over α-FE, Fe_2O_3, and Fe_3C will be compared to establish patterns in catalytic activity and selectivity as a function of catalyst composition. X-ray diffraction patterns will be taken of the fresh and spent catalysts to determine whether bulk composition changes with time on stream. In particular it would be desirable to know whether these materials achieve a common bulk composition, catalytic activity, and selectivity after extended use.

Efforts will also be made to interpret the rate data obtained for α-Fe, Fe_2O_3, and Fe_3C in the light of mechanistic models of the reaction kinetics.

The work on supported Fe catalysts will be concluded by obtaining data on the performance of Fe/Al_2O_3, Fe/TiO_2, and Fe/MgO for comparison with the data already available for Fe/SiO_2 and zeolite-supported Fe. All catalysts will be examined both in a calcined and in a reduced state to determine the influence of pretreatment. Additional work will also be done with Fe/ZSM-5 to understand better why the zeolite appears to influence the product distribution so little at temperatures below 300°C. It is conceivable that for the zeolite to have an effect, the temperatures must exceed 300°C by a substantial margin.

Task 3: CATALYZED LOW TEMPERATURE REACTION OF CARBON AND WATER

G. A. Somorjai, Task Manager

Leads to make the production of higher hydrocarbons from carbon and water truly catalytic will be pursued. It appears possible to catalytically decompose phenolates formed, preventing stoichiometric limitations.

Attempts will be made to greatly increase rates and volume of hydrocarbon formation. This may be accomplished by operation at higher water partial pressure and by catalytic promoters. Further, the addition of CO, resp. CO_2, to the reaction offers indications of producing liquidhydrocarbons.

Task 5: CHEMISTRY OF COAL SOLUBILIZATION AND LIQUEFACTION

R. H. Fish, Task Manager

The FY84 program will concentrate on the use of polymer-supported catalytic hydrogenation of model coal compounds. This will include experiements with deuterium rates, and competitive reaction to better

define potential catalyst poisoning as well as enhancement of rates of selected model coal compounds.

Catalytic cracking of partially hydrogenated nitrogen containing ring compounds will be investigated to determine the total savings of hydrogen in nitrogen removal over conventional hydrocracking.

In addition, we will attempt to define the important parameters in the catalytic transfer of hydrogen from saturated nitrogen heterocyclic compounds to other coal liquid constitutents. This will include scope, rates and a perusal of polymer-supported catalysts capable of dehydrogenation-hydrogenation reactions.

III. Highlights

Task 1: SELCTIVE SYNTHESIS OF GASOLINE RANGE COMPONENTS FROM SYNTHESIS GAS
A. T. Bell, Task Manager

1. Work on this task was completed with the submission to two Ph.D. Theses and preparation of several publications.

2. Part of this investigation has focussed on the influence of a variety of factors on the product distribution and kinetics of Fischer-Tropsch synthesis over iron catalysts in a fixed bed reactor.

   a. Activities of bulk iron catalysts decrease in the order of: P-Fe(O_x) > P-Fe(Red.) > P-K/Fe(Red.) > F-K/Fe (Red.)
   where P and F stand for catalyst preparation by precipitation or by fusion, O_x and Red. indicate pretreatment by oxidation or reduction, and K denotes potassium.
   b. Turnover frequencies of supported iron catalysts decrease in the order:
   11% Fe/TiO_2 > 20% Fe/Al_2O_3 > 11% Fe/SiO_2 > 5% Fe/Y-zeolite > 14% Fe/MgO.
   c. Major reaction products are linear hydrocarbons, principally α-olefins, β-olefins and paraffins. The production of significant amounts of β-olefins and n-paraffins is due to readsorption and further reaction of α-olefins.
   d. Promotion with potassium or the use of a basic support such as MgO prevents α-olefins from readsorbing and also increases production of CO_2 by the water-gas shift reaction.
   e. Rates of CO consumption and of production of individual hydrocarbons can be described by power law rate expressions.

3. Another part of this investigation has focussed on the kinetics

and selectivity of hydrocarbon synthesis with unpromoted bulk iron-based catalysts in a well-stirred slurry reactor which was free of temperature and concentration gradients.

a. Catalysts tested were: Fe_2O_3, fused iron, Fe_3C and Fe.
b. Activity of fused iron catalyst, increases with the extent of reduction in hydrogen, attributed to increases in surface area.
c. Main reaction products with fused iron are normal l-olefins, and paraffins, CO_2 and H_2O. The distribution follows a Schulz-Flory relationship in the range of C_1 to C_7 with a chain growth probability (α) of 0.67. The value of α is insensitive to changes in reaction conditions and the rates of hydrocarbon production are well described by power rate laws. Rates are nearly first order in hydrogen and slightly negative order in CO.
d. Kinetics and selectivity of potassium promoted Fe_2O_3 are nearly identical with those of fused iron. The value of α has a strong dependence on reaction conditions. The active catalyst for both, Fe_2O_3 and K promoted Fe_2O_3 is x-Fe_5C_2, ε'-$Fe_{2.2}C$ and perhaps Fe on Fe_3O_4. Reduced Fe_2O_3 converts entirely to carbides and Fe <u>in situ</u> and, except for lower values, has a product spectrum like untreated Fe_2O_3.
e. Fe and Fe_3C have comparable activities and selectivities but are more than 70 fold less active than Fe_2O_3. Rates of product formation depend strongly on product molecular weight and are not well described by power rate laws.

Task 3: CATALYZED LOW TEMPERATURE REACTIONS OF CARBON AND WATER
G. A. Somorjai, Task Manager

1. In the last annual report (FY 1983) it was shown that the production of hydrocarbons from graphite and water in the presence of KOH was a stoichemetric reaction. Phenolates were also formed. We have now learned that the reaction can be made truly catalytic by using certain metal oxides, such as Fe_2O_3 or NiO as co-

catalysts with KOH.

2. Using co-catalysts, the reaction proceeds continuously at temperatures below 900 K (the minimum temperature for conventional steam gasification) and produces predominantly CO_2 and H_2 according to $C+2H_2O \rightarrow CO_2+2H_2$.

3. The metal oxide co-catalysts by themselves have no reactivity for the reaction.

4. The product distribution obtained is far from equilibrium suggesting that this process is controlled by the kinetics of a surface reaction, which remains to be investigated.

5. Studies with XPS have confirmed the presence of a potassium phenolate intermediate on the surface of KOH treated graphite after reaction with steam.

6. Work has been started on surface studies in the presence of added amounts of gases, such as CO or CO_2.

Task 5: CHEMISTRY OF COAL SOLUBILIZATION AND LIQUEFACTION: Catalytic Hydrogenation of Model Coal Compounds
R. H. Fish, Task Mamager

1. A comparison between polymer-supported Wilkinson's catalyst, [P] - $P\phi_2Rh(\phi_3P)_2Cl$, and its homogeneous analogue in the selective hydrogenation of polynuclear heteroaromatic compounds provides evidence for differences in initial rates and ability to exchange aromatic hydrogens for deuterium. Cross-linking of the polymer-supported catalyst also affected hydrogenation rates, but diffusion into the polymer bead was not rate limiting. High regioselectivity for reduction of the nitrogen heterocyclic ring was found in the hydrogenation of a model coal liquid with the polymer-supported catalyst.

2. P-cresol was found to enhance the initial rate of hydrogenation of quinoline (1.6 to 2 fold) in a model coal liquid with polymer-supported (2% cross-linked) $(\phi_3P)_3RhCl$.

3. Rate studies of quinoline reduction to tetrahydroquinoline in the presence of the homogeneous catalysts $(\phi_3P)_3RhCl$ have provided definitive evidence that benzothiophene, indole, pyrrole, carbazole, thiophene, p-cresol and dibenzothiophene enhance the initial rate of hydrogenation of quinoline by a factor greater than 1.5.

4. Kinetic studies of quinoline hydrogenation showed that the rate went through a maximum as the quinoline concentration increased.

5. The binding of quinoline to the rhodium hydride, $(\phi_3P)_3RhClH_2$ was successfully established by 200 MHz ^1H nmr experiments.

6. $(\phi_3P)_3RuCl_2$ is a more active catalyst for deuterium substitution on saturated polynuclear nitrogen heterocycles than is $(\phi_3P)_3RhCl$.

7. HDN activity of zeolite catalysts using tetrahydroquinoline as a model compound provides some evidence for hydrocracking inhibition.

IV. Summary of Studies

Task 1: SELECTIVE SYNTHESIS OF GASOLINE RANGE COMPONENTS FROM SYNTHESIS GAS

A. T. Bell, Task Manager

This project was completed in FY 1984 and has resulted in two Ph.D. theses[1,2] of more than 200 pages each and containing numerous tables and figures. This work will be published in several papers now in preparation. Since it is obviously impossible to present it in any detail in this report, major conclusions are given below and in the Highlight Section of the report.

The investigations of iron-based catalysts for Fischer-Tropsch synthesis were completed during the past year. This work was aimed at understanding the effects of catalyst composition and reaction conditions on the distribution of products formed and the kinetics of their formation. Studies were conducted in both a fixed bed reactor and a well stirred autoclave, each of which was equipped with an on-line gas chromatograph for analysis of products. Since similar results were obtained with both reactors, these will be discussed together.

Six unsupported iron catalysts were examined: iron powder, precipitated iron, potassium-promoted precipitated iron, hematite (Fe_2O_3), potassium-promoted hematite, potassium-promoted fused iron (actually Fe_2O_3), and cementite (Fe_3C). In each case, the catalyst was either reduced or calcined prior to being subjected to synthesis gas. The four unpromoted catalysts exhibited very similar behaviors. Following reduction in H_2, each catalyst exhibited a very high activity for Fischer-Tropsch synthesis.

The high initial activity could not be maintained and it was observed that the activity declined to a nearly steady-state level in about 24 hr, at which point the activity was about one-tenth of that observed originaly. A linear, Schulz-Flory distribution of hydrocarbon products was observed. The probability of chain growth α increased with decreasing partial pressure of H_2, increasing partial pressure of CO, and decreasing temperature. For the range of conditions examined, α varies between 0.47 and 0.61. The products produced over each catalyst were remarkably similar, consisting primarily of α-olefins and n-paraffins. Methyl-branched α-olefins and straight-chained β-olefins were observed in lesser concentrations, as was also CH_3OH. No higher aldehydes or alcohols were observed. The proportion of paraffins and β-olefins was a strong function of gas velocity, indicating that these products are formed via secondary processes from α-olefins. X-ray analysis of the spent catalyst suggests that the active catalyst consists of the host material (e.g., Fe_3O_4, Fe, Fe_3C) on the surface of which are small particles of x-Fe_5C_2, ε'-$Fe_{2.2}C$ and Fe.

Potassium promotion resulted in a product distribution made up of two Schulz-Flory distributions crossing at n = 7 to 8. The value of α for n = 1 to 8 was virtually the same as that for the unpromoted catalyst, while that for n > 8 was noticeably greater. It was also seen that α for the light products responded to changes in reaction conditions in a manner identical to that observed for the unpromoted catalysts, while the α for the heavier products was virtually unaffected by reaction conditions.

Studies of catalyst surface area revealed that upon reduction the BET surface area of the fused iron catalyst increased, while that of precipitated iron decreased. This is understandable. In the former case, reduction results in the formation and growth of pores in the fused iron (oxide) matrix. In the latter case, reduction brings about a sintering of the iron particles.

Retention of the high initial surface area of precipitated iron could be achieved by calcining the catalyst, and then bringing it on stream without reduction. When this is done, the catalyst activity per gram of iron is tenfold higher than that observed for reduced precipitated iron, and little deactivation occurs following attainment of the maximum activity. The product distribution is identical irrespective of whether the precipitated iron catalyst is reduced or calcined prior to use.

Supported iron catalysts were prepared without potassium promotion. The specific activities of these catalysts were found to decrease in the order: Fe/TiO_2 > Fe/SiO_2 > Fe/Al_2O_3 > Fe/Y-Zeolite > Fe/MgO. The variation in activity can be attributed primarily to metal-support interactions. In all cases, the product distribution was characterized by a single value of α which was quite sensitive to reaction conditions. The magnitude of α was comparable to that for the unpromoted bulk iron catalysts.

The kinetics of hydrocarbon synthesis over all of the catalysts studied could be represented by the expression

$$R_{C_n} = R_{C_1}{}^{\alpha n-1}$$

$$= k_{C_1} P_{H_2}^{X_1} P_{CO}^{Y_1}{}^{\alpha n-1}$$

$$\alpha = \alpha (P_{H_2}, P_{CO})$$

The global activation energy was found to be constant up to 300°C. At higher temperatures the catalyst underwent deactivation due to the rapid build-up of free carbon. The temperature at which deactivation sets in could be extended slightly by raising the H_2 partial pressure.

References:

1. "Factors Influencing Kinetics and Product Distribution in

Fischer-Tropsch Synthesis over Iron Catalysts." Dissertation of William James Cannella, Chemical Engineering Department, University of California, Berkeley, 1984.

2. "Study of Fischer-Tropsch Synthesis over Iron Based Catalysts Using a Well-Stirred Reactor." Dissertation of Ronald Alan Dictor, Chemical Engineering Department, University of California, Berkeley, 1984.

Task 3: CATALYSED LOW TEMPERATURE REACTION OF CARBON AND WATER
G. A. Somorjai Task Manager with , W. T. Tysoe and J. Carrazza

Research has been concentrated in two major areas: 1) exploratory experiments using a flow reactor to discover effective catalysts for the gasification of graphite with steam; 2) studies of the interaction of different molecules with graphite using a high pressure surface science apparatus.

1. Flow Reactor Experiments

Previously[1] it was reported that the gasification of graphite with steam below 950 K, when KOH is present on the surface, ceases after the formation of 0.5 moles of H_2 per mole of KOH adsorbed. It was suggested that the reaction was limited by the formation of a stable potassium phenolate intermediate. In order to overcome this situation, work done during this year was aimed to discover a way to decompose this surface intermediate, so that the process would be carried out catalytically below 900 K.

During this year, we found that mixtures of transition metal oxides, co-adsorbed with KOH on graphite were good catalysts for the gasification of graphite with steam below 900 K. Figure 1 shows the rate of gas production at 900 K for 9 different mixtures. KOH/NiO and KOH/$FeCO_3$ presented the largest activity for this reaction; these mixtures were studied in greater detail.

While KOH adsorbed alone on graphite behaved as a reactant for the gasification of graphite with steam, NiO and $FeCO_3$ adsorbed alone (no KOH present) have no activity for this process. The fact that the mixture of them (KOH/NiO or KOH/Fe_2O_3) is a catalyst at temperatures below 900 K suggests that there is a cooperative effect between the components.

The rate of gas production for the gasification of graphite with steam at 859K, when either KOH/NiO or KOH/Fe_2O_3 were adsorbed on graphite was followed up to a graphite conversion of 24% (24 moles of CO_2 produced per mole of catalyst adsorbed on the surface). The results for NiO/KOH shown in Figure 2, Curve A. Because more than 24 turnovers of gas can be produced at 860 K, we conclude that NiO/KOH and Fe_2O_3/KOH are indeed good catalysts for the gasification of graphite with steam.

The major gas products obtained for this process in the presence of either KOH/NiO or KOH/Fe_2O_3 are H_2 and CO_2 in the ratio of H_2 to CO_2 equal to 2.2±0.5. CH_4 is initially produced in a ratio of CH_4 to H_2 equal to 0.04±0.01, but its production decreased with time up to a ratio fo CH_4 to H_2 equal to 4×10^{-3}. CO was produced at temperatures above 900 K, however, the ratio of CO to CO_2 produced was far below the value expected at equilibrium. (See Figure 3.) In general, the product distribution obtained in these experiments is far from equilibrium. This suggests that the gasification process is controlled by the kinetics of a surface reaction.

The activity of Ni metal adsorbed alone on graphite for the gasification of graphite with steam was studied in an isothermal experiment at 859 K. Figure 2 shows that the initial gas production is an order of magnitude faster than in the case of KOH and NiO co-adsorbed on graphite, but while in the last case the reaction is still going after 24% of the graphite has be gasified, the reaction stops after 11% conversion when Ni metal is present on the surface. Further work will be done to understand why the reaction stops in the presence of Ni metal.

2. UHV/High Pressure Cell

Three major studies were done using this system during the present year. The interaction of CO and CO_2 with graphite was

studied using Thermal Desorption (TDS), Auger (AES) and X-Ray Photoelectron (XPS) spectroscopies. Also the deposition of K on graphite was monitored using AES. Finally, the presence of a potassium penolate intermediate on the surface after reaction of a KOH loaded graphite sample with steam was confirmed using XPS.

a. CO and CO_2 Interaction with Graphite

Figure 4 shows TDS at masses 28 and 44 amu obtained from polycrystalline graphite exposed to $>10^8$L of CO and CO_2. Comparison of Figures 4a and 4b show that CO and CO_2 give rise to similar CO_2 desorption (mass 44) at 730 K and CO desorption (mass 28) at 1230 K. This suggests that CO and CO_2 adsorption yield similar surface species. Peaks below 500 K are present and may be attributed to "physisorbed" gas.

Figure 5 shows an XPS of an edge plane of a sample of oriented graphite exposed to $>10^8$ L of CO_2. In addition to the C 1s graphite bulk peak, new peaks are observed at chemical shifts from the graphite peak of 3.3 ± 0.2 and 4.4 ± 0.2 eV.

The peak shifted by 3.3 eV may be assigned to a carbonyl group, and the one shifted by 4.4 eV to a carboxyl group[2]. Upon heating to 850 K (above the CO_2 desorption temperature) the spectrum changes to that shown in Figure 5b so that only a peak with a chemical shift of 3.0 eV (due to a carbonyl species) remains. This peak may be removed by heating to approximately 1400 K corresponding to the desorption of CO. The 730 K peak in thermal desorption is, then, due to the decomposition of a carbonyl species. Similarly, the 1230 K peak is produced by carboxyl decomposition.

This evidence led us to suggest that both CO and CO_2 form a lactone type intermediate, when adsorbed on graphite. This intermediate is shown below.

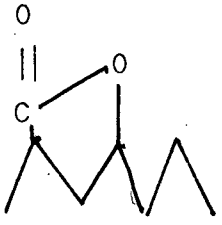

In order to decide whether peaks in the TDS spectra after CO and CO_2 adsorption (Figure 4) were indeed due to desorption from a graphite surface, a graphite single crystal with an exposed edge plane was dosed with either CO or CO_2 (>10^8L) and the KLL Augger peak-to-peak height measured as a function of annealing temperature. The results are shown in Figure 6.

Rapid decreases are observed, corresponding to either CO or CO_2 desorption. These data further confirm that peaks below 500 K are indeed due to desorption from the graphite surface.

The reaction between CO or CO_2 and polycrystalline graphite was investigated as a function of sample temperature in the high pressure reactor. For the reaction $CO_2 + C \rightarrow 2CO$ an activation of 61± 3 Kcal/mole was found. This is in good agreement with a value of 59 Kcal/mole obtained in a flow reactor[3]. For the reverse reaction, $2CO \rightarrow CO_2 + C$, and an activation energy of 24±2 Kcal/mole was found. The difference between these activation energies, i.e. the enthalpy of reaction, is 43±5 Kcal/mole, which is in good agreement with the literature value (41.2 Kcal/mole).[4]

b. Adsorption of K on Graphite

The adsorption of potassium on graphite has been studied. Figure 7 shows a 39 amu TD spectrum after exposure to potassium at room temperature. This exhibits a sharp peak at 440 K and a broad peak centered at 730 K. Loss of surface potassium during a desorption sweep can be monitored by Auger spectroscopy, and

Figure 6 also shows the amount of potassium remaining on the surface as a function of temperature. Figure 7 also is the same data obtained from thermal desorption (i.e. by integrating the TDS). There is evidently divergence between the two curves above 600 K. Below this temperature the agreement is good. This suggests that the low temperature peak is due to surface potassium while the high temperature peak is due to bulk potassium (i.e. intercalation).

This view is supported by the data of Figure 8, which shows the amount of potassium on the surface as a function of exposure. There is a break in both potassium and carbon curves indicative of the completion of one monolayer. Subsequently, the potassium signal indicates the deposition of several monolayers of potassium with only minimal attenuation of the carbon substrate signal. This result can be explained by assuming that potassium intercalates.

e. Interaction Between KOH and Graphite in the Presence of Steam

A KOH loaded graphite sample was reacted in 20 torr water vapor in the high pressure all at 800 K (the temperature at which the steam KOH/C reaction deactivates).

The spectrum of the sample in the C 1s and K 2P regions taken after this treatment is shown in Figure 9. A shoulder is visible on the C 1s peak to low binding energy after reaction. This peak is shown in Figure 9 multiplied by 4, and corresponds to a surface species within a C 1s chemical shift of 1.6 eV. This corresponds to the chemical shift of a C-O single bond. The oxygen to potassium ratio may be measured by comparison to the ratio measured for KOH. The ratio in the species after reaction is identical to KOH and so has the stoichemistry KxOx. The K 2p XPS peak position after reaction is not inconsistent with a K^{+1} species. However, since the chemical shift between a K^{+1} and K^{o}

species is small (0.5 eV) no definitive conclusions can be derived from the peak positions. However, all the data are consistent with the existence of a potassium phenolate species at the surface after reaction with steam at 800 K.

3. Future Work

The effect of adding H_2, CO, CO_2 and CH_4 to the reactant steam on the gasification of graphite with steam will be studied. These studies will tell us if the product distribution obtained when NiO/KOH are present is due to decomposition of some of the gas products or preferential formation of other gases.

Surface science studies of KOH and NiO co-adsorbed on graphite will be done before and after reaction with steam, in order to determine surface intermediates and oxidation states of the catalyst involved in the reaction.

The catalytic activity of Ni metal and NiO for other reactions related to the gasification of graphite with steam, like water gas shift and steam reforming will be studied in the UHV/high pressure system. We expect that these studies will give us some information about why the proportion of CH_4 and CO in the gas products of the gasification of graphite with steam is below the value expected at equilibrium.

Isotope experiments will be done to verify the presence of a lactone type surface species when CO or CO_2 is absorbed on graphite.

Solid state NMR studies will be done to complement the results obtained with other surface science techniques.

References:

1. F. Delannay, W.T. Tysoe, H. Heinemann and G.A. Somorjai.

Carbon, in press.

2. R. Schlogel and H.P. Boehm. Carbon, 12, 345 (1984).

3. S. Ergun. J. Phys. Chem. 60, 480 (1965).

4. Handbook of Chemstry and Physics 61st Edition. CRC Press, 1980-1981.

Figure Captions:

Figure 1: Diagram of the relative activities of various KOH co-catalyst systems.

Figure 2: Total gas production for gasification of graphite with steam as a function of time for NiO/KOH, Ni metal and KOH adsorbed on graphite.

Figure 3: Plot of the comparison between the ratio of CO and CO_2 expected at equilibrium and the ratio obtained experimentally for the gasification of graphite with steam.

Figure 4: Thermal desorption spectra obtained at 28 and 44 amu after (a) $5x10^8$L exposure of CO and (b) $5x10^8$L exposure of CO_2 onto polycrystalline graphite.

Figure 5: (a) An XPS of the graphite edge plane exposed to 10^9L CO_2 at room temperature. The spectrum of a clean surface is shown as a line (b) Spectrum after flashing to approximately 850 K.

Figure 6: KLL Auger peak to peak height as a function of sample temperature after CO and CO_2 adsorption.

Figure 7: (———) Thermal desorption of K from graphite. Potassium loss from the graphite surface as a function of

temperature, (- - -) obtained from thermal desorption data, (x x x x) obtained from AES.

Figure 8: K AES signal (o) and C AES signal (x) as a function of potassium exposure.

Figure 9: XP spectrum in the C 1s region after reaction with steam at 800 K.

Figure 1

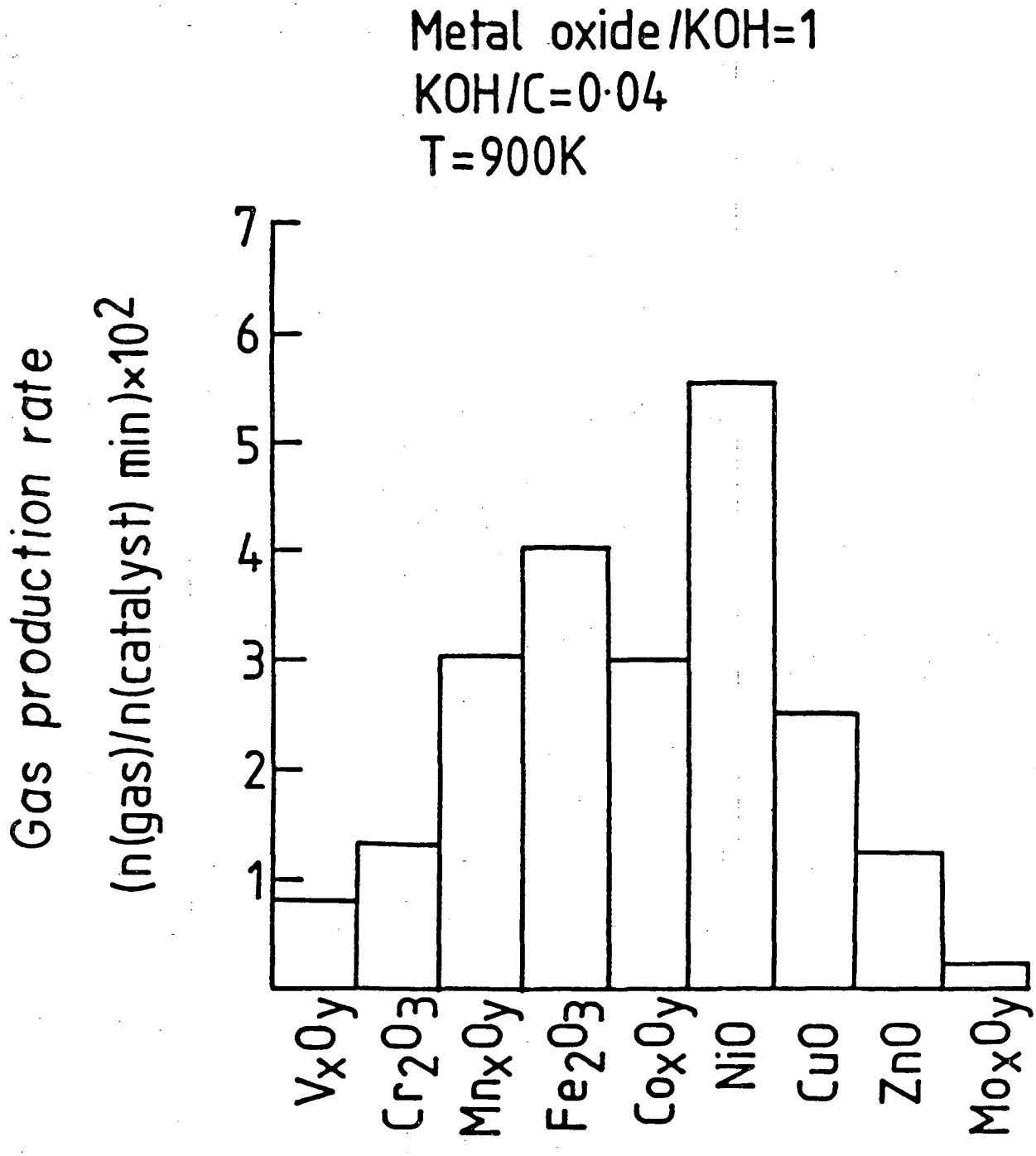
Metal oxide/KOH=1
KOH/C=0·04
T=900K
Gas production rate
(n(gas)/n(catalyst) min)×10²
7
6
5
4
3
2
1
VxOy
Cr2O3
MnxOy
Fe2O3
CoxOy
NiO
CuO
ZnO
MoxOy
XBL 848-8581

Gas production as a funtion of time

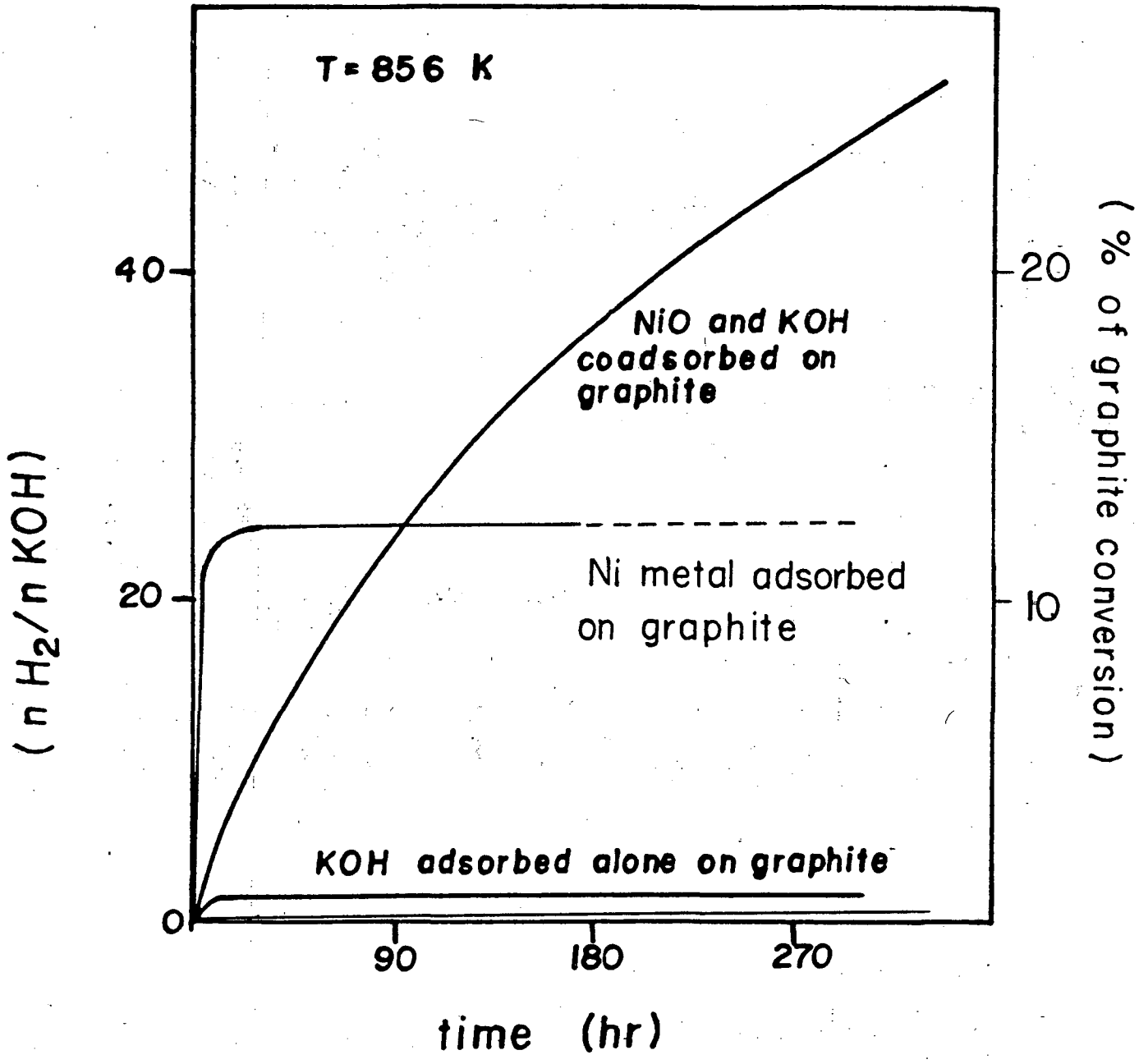

Figure 2

Figure 3

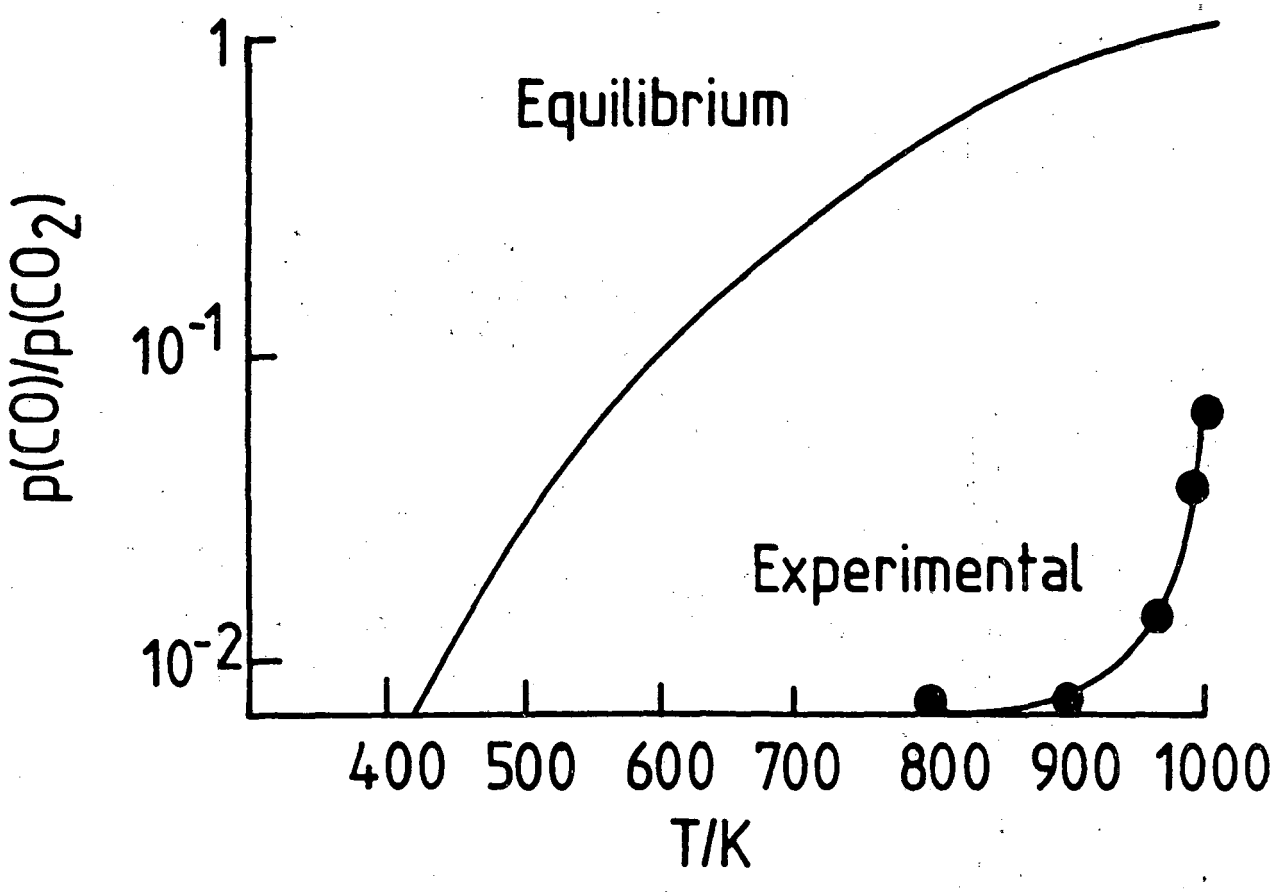
1
10^{-1}
10^{-2}
p(CO)/p(CO$_2$)
Equilibrium
Experimental
400 500 600 700 800 900 1000
T/K

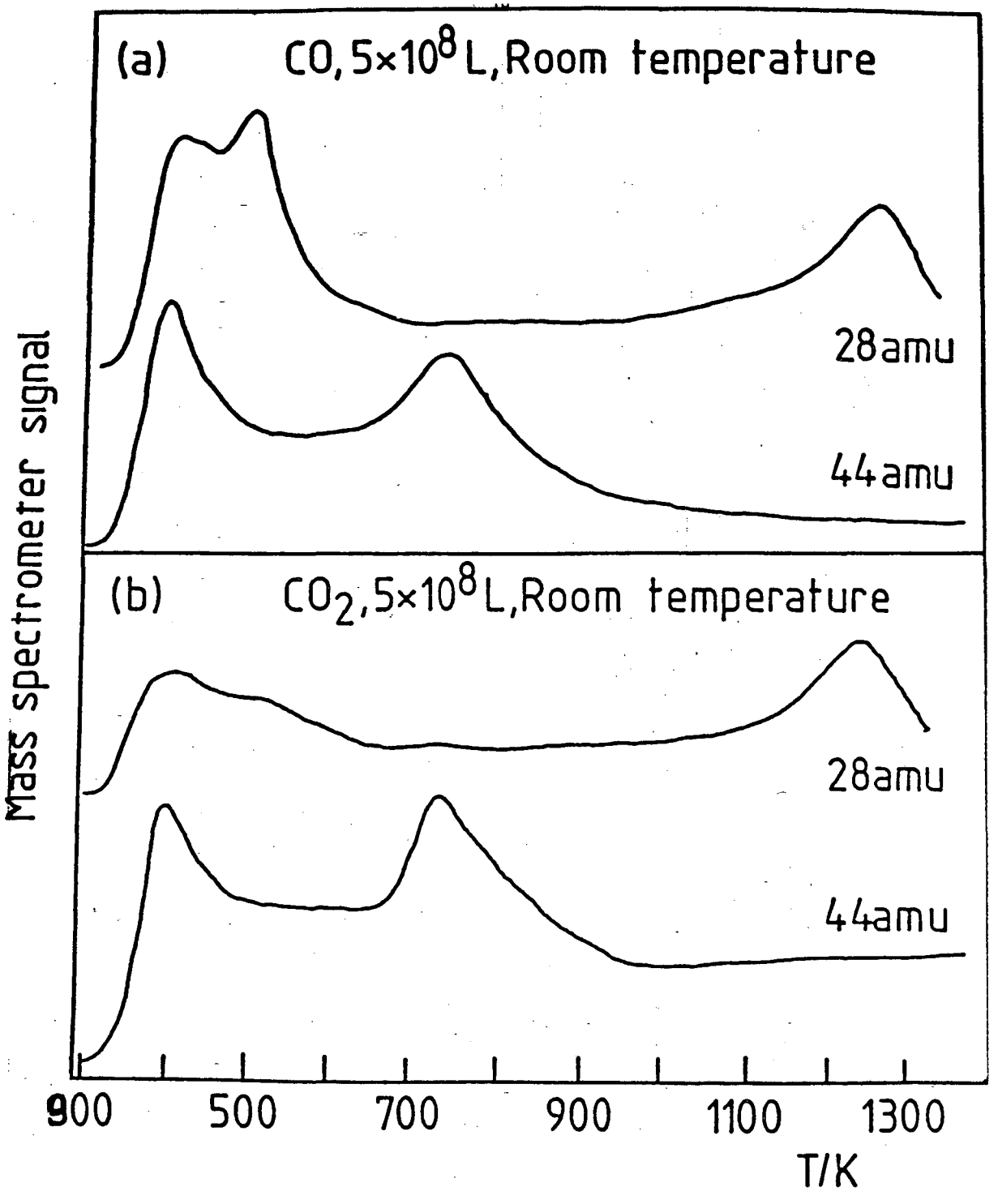
(a) CO, 5×10⁸ L, Room temperature
28amu
44amu
(b) CO₂, 5×10⁸ L, Room temperature
28amu
44amu
Mass spectrometer signal
300
500
700
900
1100
1300
T/K

Figure 4

Figure 5

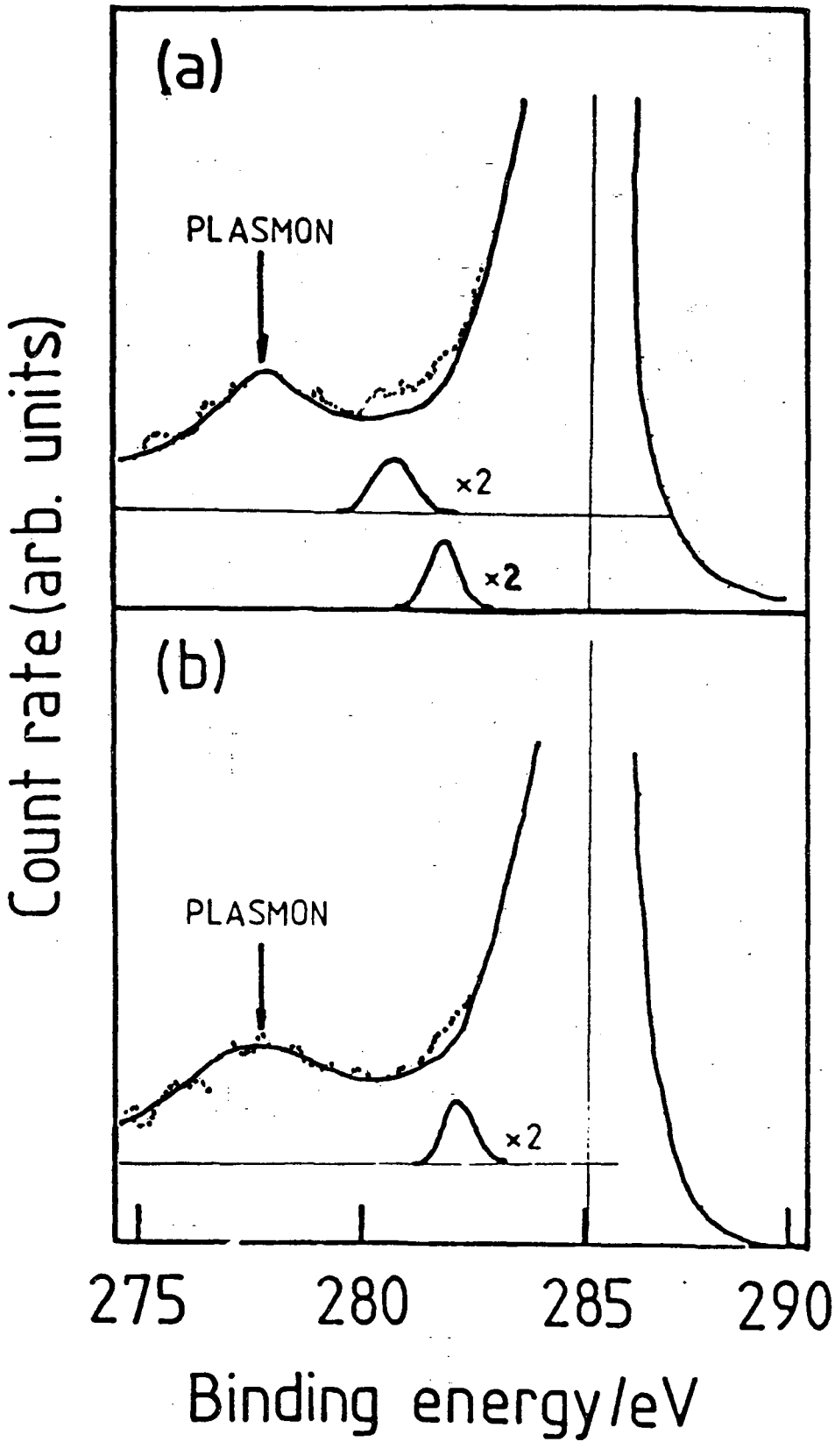
(a)
PLASMON
×2
×2
(b)
PLASMON
×2
Count rate (arb. units)
275
280
285
290
Binding energy/eV

Figure 6

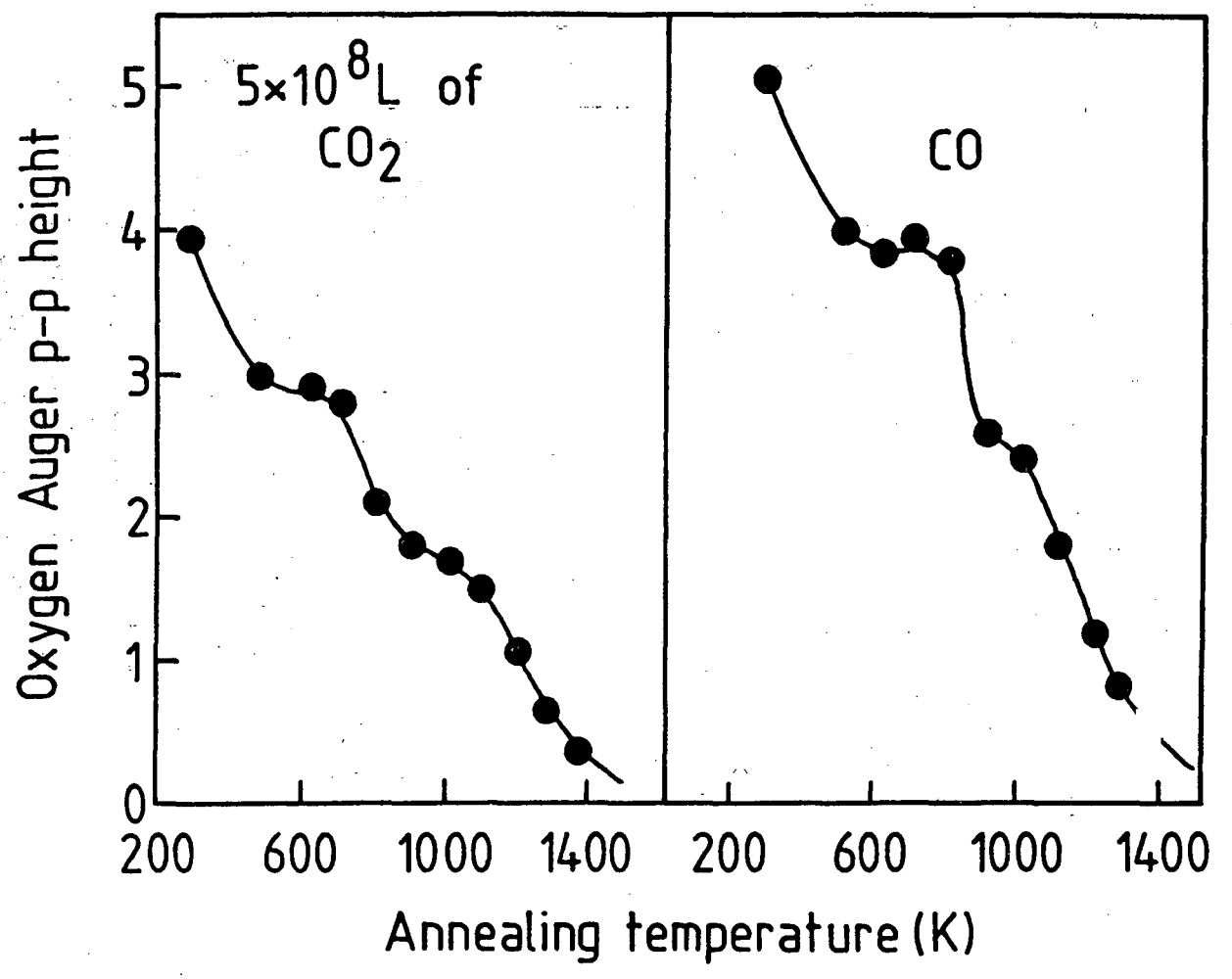
5×10⁸L of
CO2
CO
Oxygen Auger p-p height
0
1
2
3
4
5
200
600
1000
1400
200
600
1000
1400
Annealing temperature (K)

Figure 7

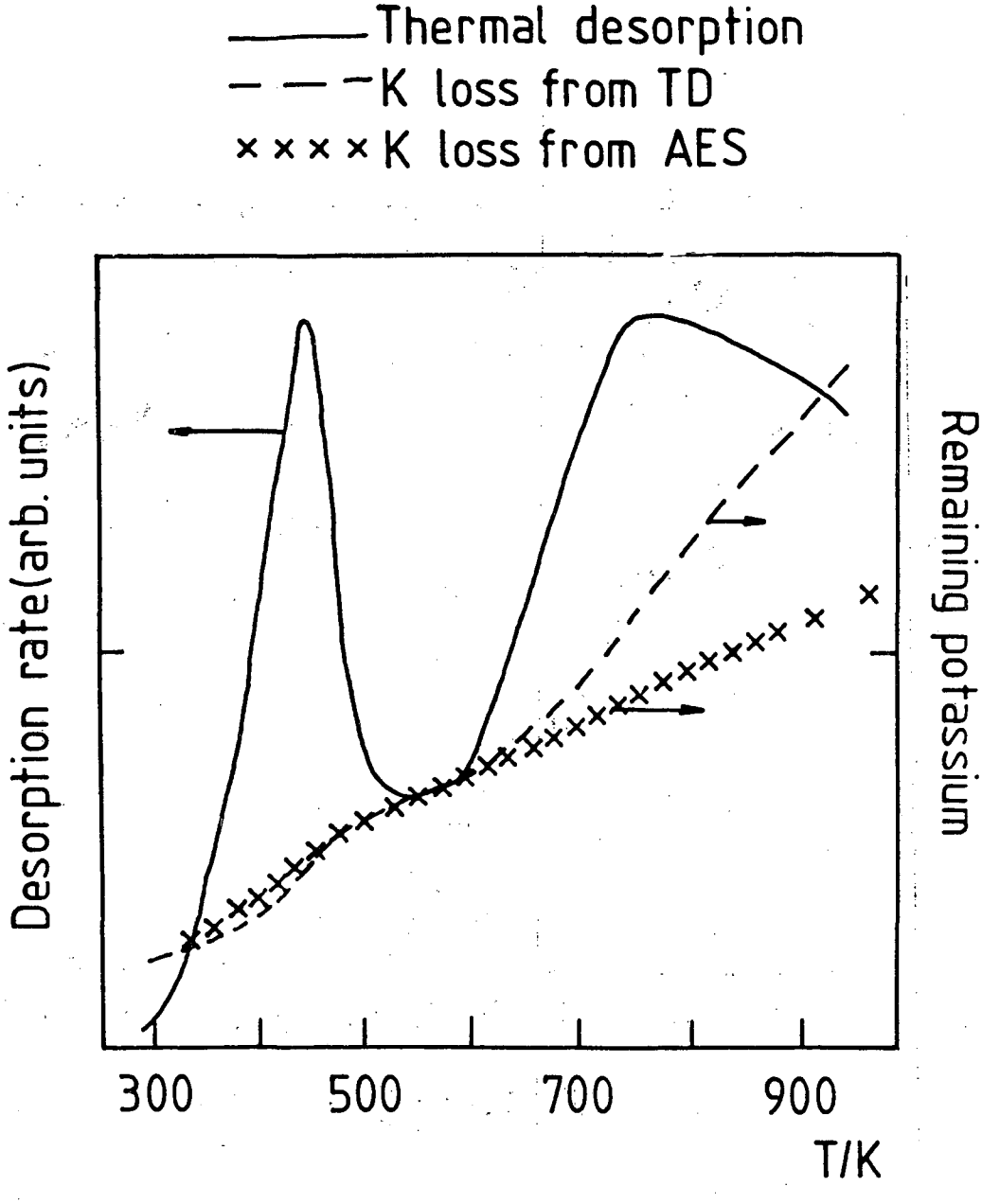
Thermal desorption
K loss from TD
K loss from AES
Desorption rate(arb. units)
Remaining potassium
300
500
700
900
T/K

Figure 8

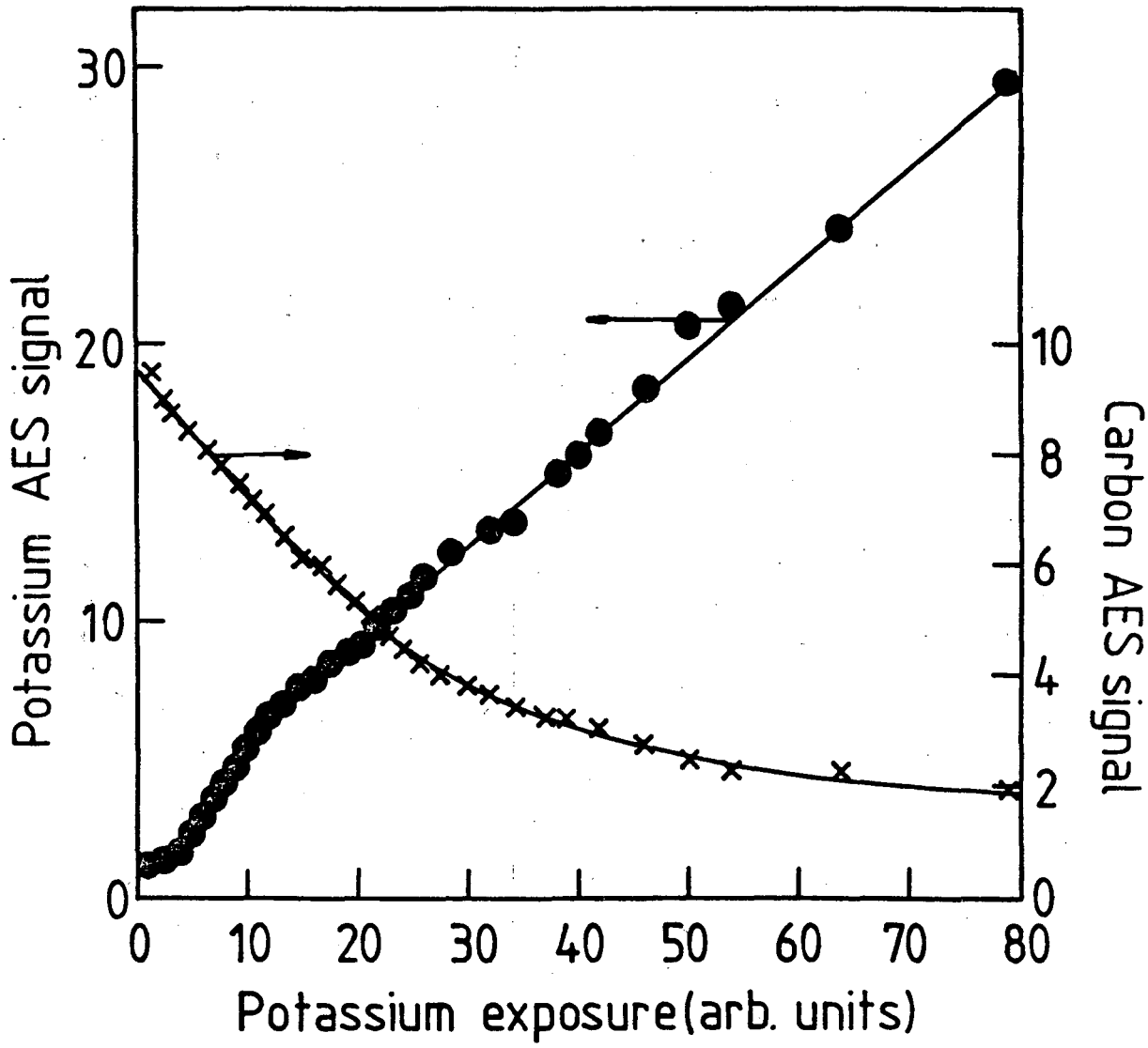
Potassium AES signal
Carbon AES signal
Potassium exposure(arb. units)
0
10
20
30
40
50
60
70
80
0
2
4
6
8
10
0
10
20
30

Figure 9

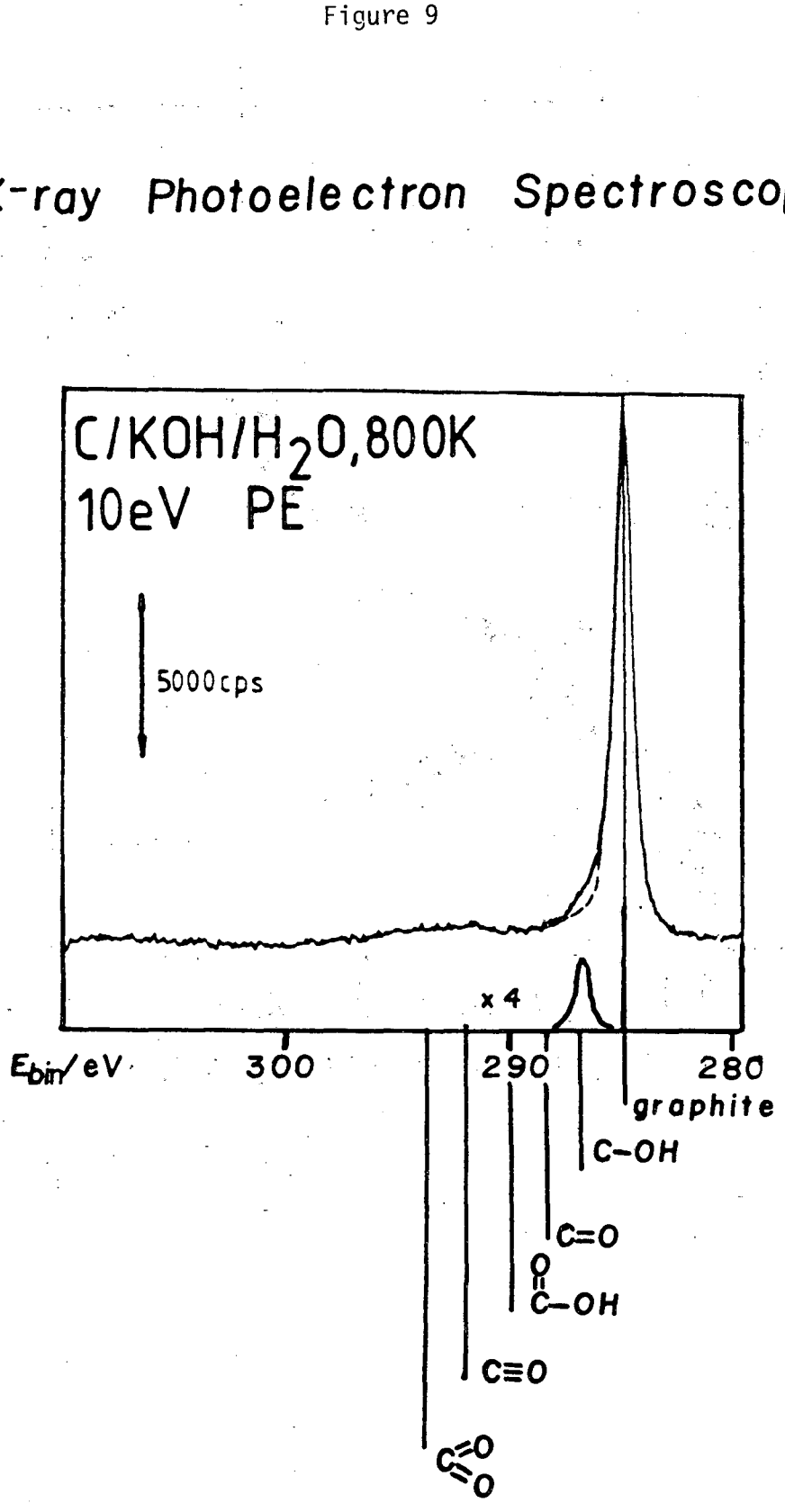
X-ray Photoelectron Spectroscopy
C/KOH/H2O,800K
10eV PE
5000cps
x 4
Ebin/eV
300
290
280
graphite
C-OH
C=O
O
C-OH
C≡O
C=O
O

Task 5. CHEMISTRY OF COAL SOLUBILIZATION AND LIQUEFACTION
R.H. Fish Task Manager with A.D. Thormodsen

Polymer-Supported Catalysts in the Selective Reduction of Model Coal Compounds

We report on our results of a comparison of polymer-supported Wilkinson's catalyst on 2% cross-linked phosphinated polystyrene-divinylbenzene (PS-DVB) with results obtained with the homogeneous analogue for the selective reduction of polynuclear heteroaromatic nitrogen and sulfur compounds.

Initial and Relative Rates

The initial and relative rates of reduction of the substrates were obtained using a Parr kinetic apparatus. Table 1 indicates the results of this coomparison, with substrate to metal ratio, temperature, and partial pressure of hydrogen being equivalent for both forms of Wilkinson's catalyst. The polymer-supported catalyst results in Table 1 were carried out with the same batch of 2% PS-DVB beads with excellent reproducibility upon repetition of each experiment.

Several important observations become apparent from these results; namely, the initial rates of hydrogenation of the nitrogen heterocyclic compounds studied with polymer-supported Wilkinson's catalyst are 10-to-20 times faster than the homogeneous equivalent. This unusual enhancement is extremely relevant for practical applications and has not been observed with many polymer-supported catalysts in other reduction reactions.

Several reasons for the rate enhancement of the polymer-supported over the homogeneous catalyst can be formulated. One important consideration may be found in the fact that the substrates are

themselves suitable ligands. Also, a higher concentration or enrichment of substrate around the polymer-supported metal center, with concomitant loss of triphenylphosphine, may be of consequence in these rate enhancements. Other factors such as steric and electronic effects are also probably involved. For example, the relative rate differences between the compounds studied for both forms of Wilkinson's catalyst may involve steric effects as accentuated by the 5,6 and 7,8-benzoquinoline rate ratio 2/3 = 6.0 as well as the quinoline-benzoquinoline rate ratios of 2 and 13 respectively. It is interesting to note that only in the case of the sulfur heterocyclic compound is the initial rate larger for the homogeneous catalyst, while overall relative rates are similar for the nitrogen compounds within each set of catalyst results.

Selectivity

The high regioselectivity for the heteroaromatic ring, with both forms of the catalyst, is evident (Table 1). In one case (acridine), the polymer-supported catalyst gave only 9,10-dihydroacridine with no 1,2,3,4-tetrahydroacridine apparent. In contrast, the homogeneous analogue gave substantial amounts of the outer ring product (approx. 50%) and this difference may result from the more pronounced steric requirements surrounding the active metal sites on the polystyrene-divinylbenzene supported catalyst.

Parameters that Affect Rate

Several other parameters that were critical to study included the effect of cross-linking and diffusion rates of substrate into the PS-DVB beads. In experiments to clarify these points, the 2% cross-linked polystyrene-divinylbenzene beads with Wilkinson's catalyst were compared to the 20% cross-linked beads for reduction of quinoline and the initial rate ratio for both (2%/20%) was found to be approximately 3. We also ground the 2% beads and hydrogenated quinoline using similar reaction conditions to show that diffusion of substrate into the bead was not rate limiting, i.e., both ground and whole (approx.

30 μ) 2% cross-linked beads gave the same initial rates within experimental error.

Mechanism of Hydrogenation of Quinoline with Polymer-Supported Wilkinson's Catalyst

The mechanism of reduction of quinoline with deuterium gas was recently elucidated with homogeneous Wilkinson's catalyst. In that study, we found the following pattern of deuterium incorporation as shown, 6.

In contrast, compound 7 shows the deuterium pattern (nmr and ms) obtained with 2% corss-linked PS-DVB Wilkinson's catalyst. The pertinent difference is the lack of aromatic C-H exchange (C_8)

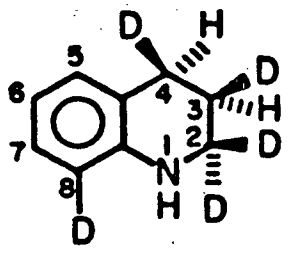

6

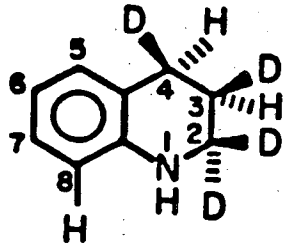

7

for the polymer-supported catalyst, while stereochemistry at the 3,4-double bond (cis) and reversible dehydrogenation of the reduced carbon-nitrogen bond (positions 1 and 2) to provide 1.6D at the 2-position, via quinoline-2-d, is similar for both forms of the catalyst. Moreover, reaction of the product, 1,2,3,4-tetrahydroquinoline, with PS-DVB Wilkinson's catalyst under similar deuteration conditions also shows, by nmr and ms analysis, no exchange of the aromatic hydrogen at position 8 (6.42 ppm), and is in contrast to the homogeneous catalyst result. Again, steric requirements surrounding the polymer-supported catalyst active metal center may be responsible for the lack of aromatic C-H exchange.

Reduction of Quinoline in the Presence of Model Coal Liquid Constituents

Since the compounds shown in the Table 1 are prevalent in synthetic fuel products such as coal liquids, we wanted to determine whether the selectivity for the nitrogen heterocyclic ring (with quinoline as the example) would prevail in the presence of other coal liquid constituents. The model coal liquid, disolved in benzene and containing (wt%) 30% pyrene, 5% tetralin, 38% methylnaphthalene, 17% m-cresol, 7.5% quinoline and 2.5% x-methylpyridine, was hydrogenated with the 2% PS-DVB Wilkinson's beads (similar conditions as shown in Table 1) to provide 1,2,3,4-tetrahydroquinoline as the only reduction product (initial rate 0.42%/min). Removal of 2-methylpyridine had no effect on the initial rate in contrast to the competitive inhibition on quinoline by the pyridine derivative in the homogeneous reaction. Interestingly, reduction of quinoline alone, at a similar substrate-to-metal ratio as in the model coal liquid, provided an initial rate (0.18%/min) that was approximately 2.2 times slower than the rate of quinoline in the presence of the model coal liquid constituents.

We have been able to confirm that p-cresol, a constituent in a model coal liquid containing pyrene (30% by wt.), tetralin (5%), methylnaphthalene (38%), p-cresol (17%), quinoline (7.5%), and methylpyridine (2.5%) enhances the rate of quinoline hydrogenation by a factor of approximately two. In addition, 2-methylpyridine had no effect on the quinoline reduction rate, which is in contrast to its effect when using a homogeneous catalyst. Thus, p-cresol might be useful in the hydroprocessing of coal liquids.

The above-mentioned result emphasizes the highly selective reaction taking place in the presence of other functionalities, i.e. regiospecific reduction of the nitrogen heterocyclic ring as well as the rate enhancement phenomena, and provides dramatic evidence for the potential usefulness of polymer-supported catalysts in synthetic fuel (hydroprocessing) applications.

Homogeneous Catalytic Hydrogenation of Model Coal Compounds

Kinetics of Quinoline Hydrogenation

The detailed kinetics of the reduction of a model coal compound, quinoline, was initiated. The rate of reaction was found to go through a maximum as the quinoline concentration was increased (Figure 1). Thus, quinoline acts as an inhibitor during the hydrogenation reaction at and above the substrate to catalyst ratios (>10:1) we have been using in our previous experiments.

Rate Enhancement Studies of Quinoline Hydrogenation with Homogeneous $(\phi_3P)_3RhCl$ as a Catalyst

We studied the relative rates of hydrogenation of quinoline in the presence (1:1) of other heteroaromatic compounds to ascertain the scope of the rate enhancement phenomena we discovered previously. We found that benzothiophene, indole, pyrrole, carbazole and thiophene had enhanced the relative rate of quinoline hydrogenation by a factor of 1.5 (quinoline alone = 1.0), while dibenzothiophene and p-cresol increased the quinoline hydrogenation relative rate by a factor of 1.8 and 2.5 respectively. We believe this increase in relative rate is caused by either a more favorable pathway for coordination of quinoline to the rhodium metal center in the presence of the above mentioned compounds or alternatively that they act as ligands to stabilize electron deficient rhodium metal centers.

Quinoline Binding to $(\phi_3P)_3RhClH_2$

In order to provide information concerning the binding of quinoline to a rhodium metal center, we utilized a 200 MHz ^1H nmr spectrometer for these studies and found that indeed quinoline failed to bind to $(\phi_3P)_3RhCl$. However, if we preformed the rhodium hydride, $(\phi_3P)_3RhClH_2$, we found that the protons at the 2 and 8 positions of quinoline were shifted to lower field by 0.13 and .09 ppm. This experiment provides definitive evidence that the "hydride route" is

favored, i.e., H oxidatively adds first, followed by loss of triphenylphosphine, and then quinoline oxidatively adds to the rhodium metal center. These results confirm our previously postulated binding mechanism in the total scheme of quinoline hydrogenation.

Comparison of $(\phi_3P)_3RuCl_2$ to $(\phi_3P)_3RhCl$ in the Mechanism of Hydrogenation of Quinoline

We carried out several deuterium experiments in order to compare the mechanism of the reduction of the nitrogen ring in quinoline with dichloro(tristriphenylphosphine)Ruthenium (II), $(\phi_3P)_3RuCl_2$, to that previously defined with the rhodium analog, $(\phi_3P)_3RhCl$.

The results were similar with both the ruthenium and rhodium analogues (see structure 6, page 31), however, the ruthenium catalyst was able to deuterate the alpha methylene position in tetrahydroquinoline, while the rhodium catalyst was totally inactive in this reaction (Equation 1). The position of deuterium substitution was determined by both 200 MHz ^1H nmr spectroscopy and mass spectrometry.

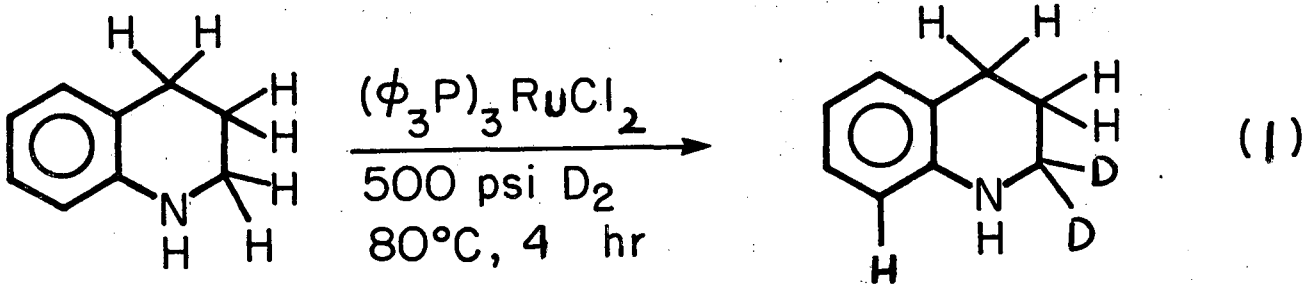

(1)

HDN Activity with a Zeolite Cracking Catalyst, Undecane as a Hydrogen Donor Source and 1,2,3,4-Tetrahydroquinoline as the Model Nitrogen Compound

The previous mentioned studies clearly defined, with various homogeneous and polymer-support transition metal compounds, that regioselective reduction of the nitrogen containing ring in

polynuclear heteroaromatic nitrogen compounds could be readily achieved.

The next step in our program (FY 85) is to more clearly understand the chemistry associated with nitrogen removal from the saturated nitrogen rings in the above mentioned model coal compounds. In view of this, we initiated some experiments using a quartz tube reactor and a zeolite cracking catalyst.

The purpose of these experiments was to evaluate, the hydrogen donor activity of a long chain paraffin, undecane, in its ability to transfer hydrogen to THQ in the presence of a zeolite industrial fluid cracking catalyst.

In preliminary experiments to ascertain cracking activity of undecane, with a zeolite catalyst, we ran our quartz reactor (480^{o}C) with undecane and found that the % cracking (via gas chromatography analysis) was over 80%. However, when we ran experiments (480^{o}C) with THQ in the presence of undecane (1 to 4 by volume) we found that undecane cracking was almost totally inhibited. These results seem to indicate that THQ has reacted with the acidic sites of the zeolite catalyst, thus, preventing undecane cracking activity.

We will try to further understand these results in future HDN experiments due to begin in FY 85.

Accepted Publications 1984

1. R. H. Fish, J.L. Tan, and A.D. Thormodsen. Homogeneous Catalytic Hydrogenation 2. Selective Reductions of Polynuclear Heteroaromatic Compounds Catalyzed by Chloro(tristriphenylphosphine)Rhodium (I). J. Org. Chem. (in press).

2. R. H. Fish, A.D. Thormodsen, and H. Heinemann. A Comparison of Polymer-Supported Chloro(Tristriphenylphosphine)Rhodium (I) to its Homogeneous Analogue in the Selective Reduction of Polynuclear

Heteroaromatic Compounds. J. Mol. Catal. (in press).

Figure Caption

Figure 1: Plot of the quinoline reduction rate versus the concentration of quinoline in the conversion to 1,2,3,4-Tetrahydroquinoline.

Table 1

Comparison of Initial and Relative Rates of Hydrogenation of Substates 1-5 Using Both Polymer-Supported and Homogeneous Wilkinson's Catalysis[a]

Substrate	Product[b]	Polymer-Supported Rates[c] Initial (%/min)	Relative	Homogeneous Rates Initial (%/min)	Relative	PS/H Rate Ratio
Quinoline	1,2,3,4 Tetrahydro-	.29	1	.013	1	22
5,6 Benzoquinoline	1,2,3,4 Tetrahydro-	.14	.48	.0065	.5	22
7,8 Benzoquinoline	1,2,3,4 Tetrahydro-	.024	.08	.0012	.09	20
Acridine	9,10 dihydro-	~.4	~1.4	~.04	~3	10
Acridine	1,2,3,4 Tetrahydro-	0	0	.047	3.6	0
Benzothiophene	2,3 Dihydro	~.03	~.1	.044	3.4	.7

a) Reaction conditions were as follows: P_{H2}=310 psi, T=85°C, sub./Cat.=91/1, Benzene (20 ml), 1 mmole substrate in each case, with either 10.2 mg of homogeneous $RhCl(PPh_3)_3$ or 52 mg of polymer-supported Wilkinson's catalyst [2% cross-linked, 2.19% Rh, initial P/Rh=2.9 (Strem Chemical Co.), P/Rh after reaction with substrate 1-5 ~3.3] contained in a wire basket attached to the end of the dip-tube of the kinetic apparatus.

b) Analysis by gas chromatography.

c) Plots of % conversion vs. time provided initial (pseudo zero order) rates. Rates are relative to quinoline (1.0). Substrates, 1-5, were reacted with the same beads for all initial rates reported.

Figure 1

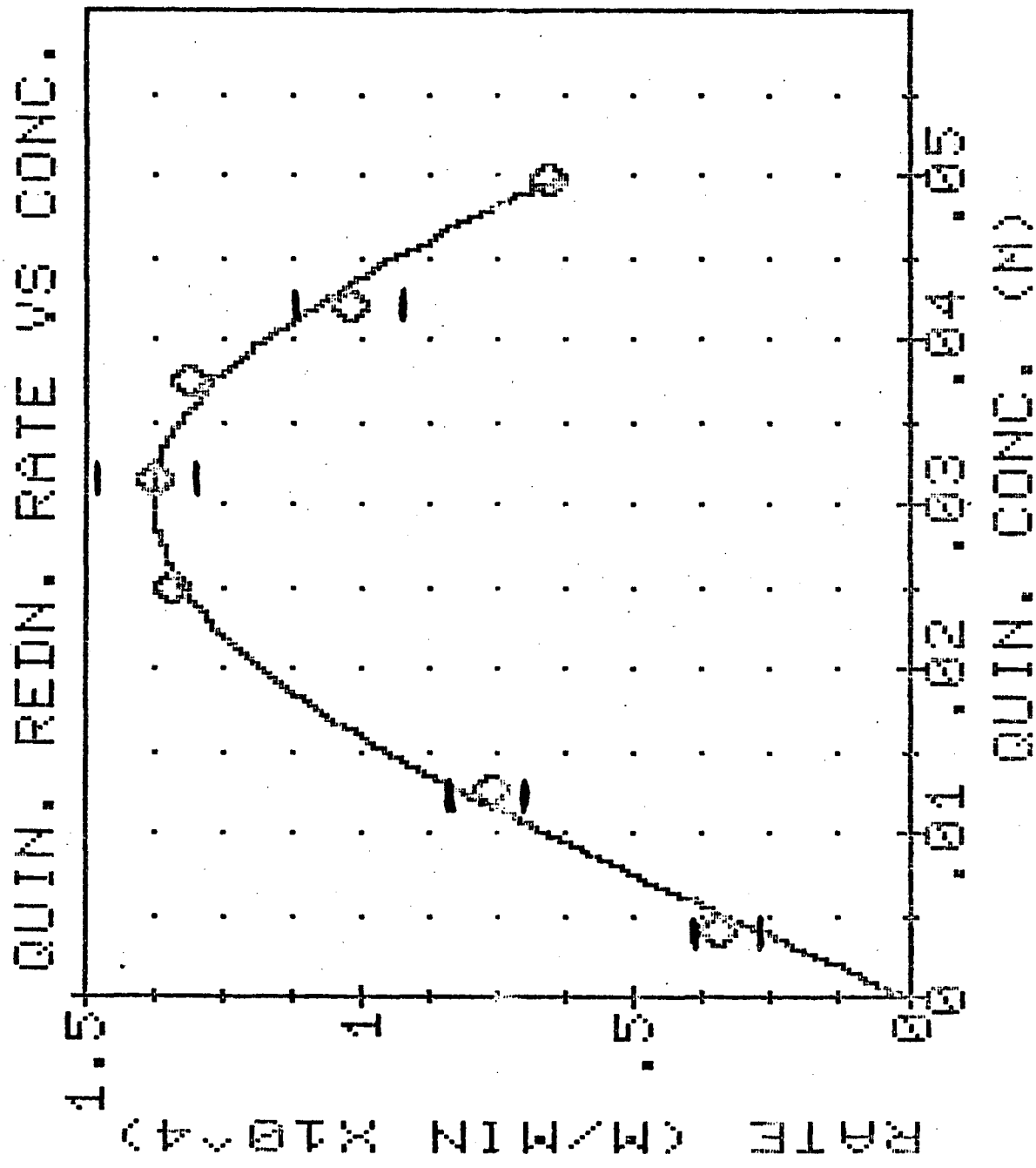
QUIN. REDN. RATE VS CONC.
RATE (M/MIN X10^-4)
QUIN. CONC. (M)
1.5
1
.5
0
0
.01
.02
.03
.04
.05

This report was done with support from the Department of Energy. Any conclusions or opinions expressed in this report represent solely those of the author(s) and not necessarily those of The Regents of the University of California, the Lawrence Berkeley Laboratory or the Department of Energy.

Reference to a company or product name does not imply approval or recommendation of the product by the University of California or the U.S. Department of Energy to the exclusion of others that may be suitable.

TECHNICAL INFORMATION DEPARTMENT
LAWRENCE BERKELEY LABORATORY
UNIVERSITY OF CALIFORNIA
BERKELEY, CALIFORNIA 94720